LIQUID-PHASE AXIAL DISPERSION IN A PACKED GAS ABSORPTION COLUMN

Richard A. Davis, Joe H. Doyle,
Orville C. Sandall
University of California
Santa Barbara, CA 93106

The cost of electronic instrumentation has come down recently as a result of newer technologies and lower computer prices. We have taken advantage of this trend to create new and dynamic experiments using existing steady-state experiment apparatus. Our purpose was to enhance the learning process by removing some of the data-collection tedium and thereby leaving more time for experimental design and analysis.

One of our upgraded experiments is a packed-column apparatus used for the absorption of CO_2 into water. The column was instrumented with conductivity probes to indirectly measure inlet and exit liquid-phase concentrations. Large amounts of real-time data are readily acquired with the aid of a computer. For example, accurate unsteady-state and steady-state operations are easily observed. It is common to assume plug-flow conditions when analyzing mass transfer in a packed column. This paper presents an experiment and analysis to examine the validity of this assumption in the liquid phase.

In the first part of the experiment, the residence time distribution (RTD) of the liquid phase is determined by measuring the exit response to an impulse concentration perturbation on the liquid feed. The second half of the experiment consists of determining the overall liquid-phase mass transfer coefficient from gas-absorption measurements in the packed column. The results from the RTD experiments are used in a dispersion model to account for deviations from plug flow (*e.g.*, back mixing in the liquid phase). Dispersion effects on mass transfer are evaluated by comparing mass transfer coefficients calculated assuming plug flow with mass transfer coefficients calculated from non-ideal flow conditions. This new approach adds a degree of difficulty to the experiment by removing the plug-flow constraint and provides a setting wherein students can make critical judgements on a well-known solution.

THEORY

A model of dispersion in the liquid phase is developed for flow without interphase mass transfer to obtain a dispersion coefficient. The results are used in a second model which accounts for dispersion with interphase mass transfer in a packed column. A model for the limiting case of plug flow is also presented.

Dispersion Model

Levenspiel[1] presents the dispersion model for deviations from plug flow in the axial direction as

$$\frac{\partial C}{\partial t} = E\frac{\partial^2 C}{\partial z^2} - u\frac{\partial C}{\partial z} \qquad (1)$$

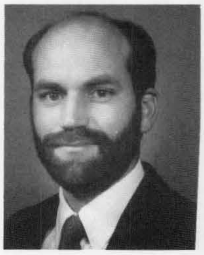

Richard Davis *received his BS degree in chemical engineering from Brigham Young University and his PhD from the University of California, Santa Barbara. He is a member of the chemical engineering faculty at the University of Minnesota, Duluth. His research and teaching interests are in the areas of separation processes and environmental remediation.*

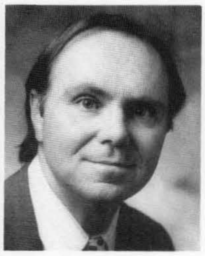

Joe Doyle *holds a BS in chemistry from UCSB and is a Development Engineer in its Chemical and Nuclear Engineering Department. His interests include analytical instrumentation, data-acquisition systems, and exploration of the world's largest aqueous sodium chloride reactor.*

Orville Sandall *is a professor in the Chemical and Nuclear Engineering Department at UCSB. He is a graduate of the University of Alberta (BSc, MSc) and the University of California, Berkeley (PhD). His teaching and research interests are in the areas of mass transfer and separation processes.*

where C = concentration
t = time
z = axial coordinate
u = superficial liquid velocity
E = dispersion coefficient which characterizes convective back-mixing as well as diffusion

Usually, the dispersion coefficient is much larger than the diffusion coefficient. Eq. (1) can be made dimensionless as follows:

$$\frac{\partial \mathbf{C}}{\partial \theta} = \left(\frac{E}{uh}\right)\frac{\partial^2 \mathbf{C}}{\partial z^{*2}} - \frac{\partial \mathbf{C}}{\partial z^*} \tag{2}$$

where the quantity

E/uh = the dispersion number (=1/Pe)
h = the length of the column.

The dimensionless variables are

$$\theta = \frac{t}{\tau} \tag{3}$$

where τ is the mean residence time

$$\tau = \frac{h}{u} \tag{4}$$

and

$$z^* = \frac{z}{h} \tag{5}$$

The concentration is normalized such that

$$\mathbf{C} = \frac{C}{Q}$$

where

$$Q = \int_0^\infty C\,dt \tag{6}$$

Thus we have

$$\int_0^\infty \mathbf{C}\,dt = 1 \tag{7}$$

Eq. (2) is examined for two regimes: small and large extents of dispersion.

For an impulse perturbation of tracer on a fluid with little dispersion, the shape of the tracer curve does not change significantly from the point of injection to the measurement point. The **C** curve at the measurement point is a Gaussian distribution.

$$\tau\mathbf{C} = \frac{1}{2\sqrt{\pi\left(\frac{E}{uh}\right)}}\exp\left[-\frac{(1-\theta)^2}{4\left(\frac{E}{uh}\right)}\right] \tag{8}$$

The dispersion coefficient can be obtained by two relatively simple methods. First, at the mean residence time, $\theta = 1$ and the **C** curve reaches a maximum. Eq. (8) may be solved for the dispersion number in terms of $\mathbf{C}_{max}$

$$\frac{E}{uh} = \frac{1}{4\pi}\left(\frac{1}{\tau C_{max}}\right)^2 \tag{9}$$

In a second method, the variance of the **C** curve can be expressed in terms of the dispersion number

$$\frac{\sigma^2}{\tau^2} = 2\left(\frac{E}{uh}\right) \tag{10}$$

The variance is defined as

$$\sigma^2 = \int_0^\infty t^2\,\mathbf{C}\,dt - \tau^2 \tag{11}$$

The solution for the dispersion number is found by rearranging Eq. (10) to give

$$\frac{E}{uh} = \frac{\sigma^2}{2\,\tau^2} \tag{12}$$

For small extents of dispersion, the experimental procedure and analysis are straightforward because the shape of the **C** curve is insensitive to the boundary conditions imposed on the packed column.

A characteristic of large extents of dispersion is an unsymmetrical response to an impulse perturbation about the mean residence time. The **C** curve typically has an extended tail. In this case, the boundary conditions become important. The current experimental setup in our laboratory is best described by closed boundary conditions (*i.e.,* the flow pattern changes abruptly at the boundaries). In this case, there is no analytical solution for the **C** curve. The variance of the **C** curve is given as

$$\frac{\sigma^2}{\tau^2} = 2\left(\frac{E}{uh}\right) - 2\left(\frac{E}{uh}\right)^2\left\{1-\exp\left[-\left(\frac{uh}{E}\right)\right]\right\} \tag{13}$$

The dispersion number may be found by determining the variance as defined by Eq. (11) and then solving the non-linear Eq. (13) for E/uh by Newton's iterations. Good initial guesses for E/uh can be obtained by using Eqs. (9) and (12) to solve for E/uh. Levenspiel[2] offers the following estimates for the extent of dispersion:

small: E/uh < 0.01 large: E/uh > 0.01

Tanks-In-Series

Levenspiel[1] also presents the tanks-in-series (TIS) model to account for deviations from plug flow conditions. In this model, the liquid flows through a series of n completely mixed stirred tanks. The **C** curve for this model is

$$\tau\mathbf{C} = \frac{(\theta n)^n}{\theta(n-1)!}\exp(-\theta n) \tag{14}$$

The number of tanks can be determined from the value for $\mathbf{C}_{max}$

$$\tau\mathbf{C}_{max} = \frac{n(n-1)^{n-1}}{(n-1)!}\exp(1-n) \cong \frac{n}{\sqrt{2\pi(n-1)}} \quad \text{for } n > 5 \tag{15}$$

A simpler technique uses the value of θ_{max}

$$n = \frac{1}{1-\theta_{\max}} \tag{16}$$

The dispersion number is related to the number of tanks as

$$\frac{E}{uh} = \frac{1}{2n} \tag{17}$$

Differential Model with Dispersion

King[3] discusses a differential model which includes dispersion effects for a stripping column in counter-current flow. A simplified version of this model for absorption is developed here. The current experimental apparatus limits the study of dispersion effects to the liquid phase. Thus, the experiments are designed so that dispersion in the gas phase is unimportant. This is accomplished by using 100% CO_2 in the gas phase for absorption experiments. Thus, the mole fraction of CO_2 in the gas phases remains constant for our experimental design. An idealized picture of the flow conditions in a counter-current gas-liquid absorption column is shown in Figure 1.

A shell balance around a differential element of the column gives the transport equation for the liquid phase as

$$LC_L \frac{dx}{dz} + EAC_L \frac{d^2x}{dz^2} + K_L aA(x_e - x) = 0 \tag{18}$$

where L = volumetric liquid flow rate
K_L = overall liquid phase mass transfer coefficient
a = effective interfacial area per unit volume
A = cross-sectional area of the column
C_L = concentration of the liquid phase
x = mole fraction of the solute in the liquid stream at position z

For the small mass transfer rates considered here, it is assumed that G, L, C_L, and K_L are constant. The subscript e indicates equilibrium conditions. If the equilibrium relationship between the phases is linear (which is the case for our system of dilute CO_2 in water) then x_e can be replaced by the equilibrium relationship

$$y = mx_e \tag{19}$$

The boundary conditions are discussed in Lo, *et al.*[4] At the liquid entrance, the net axial solute transport away from the upper boundary is equated with the solute feed into the boundary

$$LC_L x_f - EAC_L \frac{dx}{dz} = LC_L x \tag{20}$$

where the subscript f indicates feed conditions. Eq. (20) can be written as

$$\left(x_f - x\right) = \frac{EA}{L}\frac{dx}{dz} \qquad \text{at } z = h \tag{21}$$

The same argument as above leads to a similar condition at the liquid exit boundary

$$\left(x - x_0\right) = \frac{-EA}{L}\frac{dx}{dz} \qquad \text{at } z = 0 \tag{22}$$

The left- and right-hand sides of Eq. (22) are of opposite sign. Thus, Eq. (22) is only valid for the case where $x = x_0$. This result is summarized as follows

$$\frac{dx}{dz} = 0 \qquad \text{at } z = 0 \tag{23}$$

The balance is made dimensionless as follows (noting that, for the case considered here, x_e is constant since pure CO_2 is absorbed)

$$\frac{dX}{dw} + \frac{1}{Pe}\frac{d^2X}{dw^2} - NX = 0 \tag{24}$$

where

$$X = x_e - x \tag{25}$$

$$w = \frac{z}{h} \tag{26}$$

$$Pe = \frac{Lh}{EA} = \frac{uh}{E} \tag{27}$$

$$N = \frac{K_L ahA}{LC_L} \tag{28}$$

The dimensionless boundary conditions are

$$\frac{dX}{dw} = 0 \qquad \text{at } w = 0 \tag{29}$$

$$Pe(X_f - X) = \frac{dX}{dw} \qquad \text{at } w = 1 \tag{30}$$

The Peclet number, defined in Eq. (27), is the inverse of the dispersion number in Eq. (2). Note also that, as $Pe \to \infty$, the transport equation reduces to the plug-flow equation.

Equation (24) is linear and homogeneous and can be conveniently solved by the method of undetermined coefficients. From inspection of Eq. (24), the

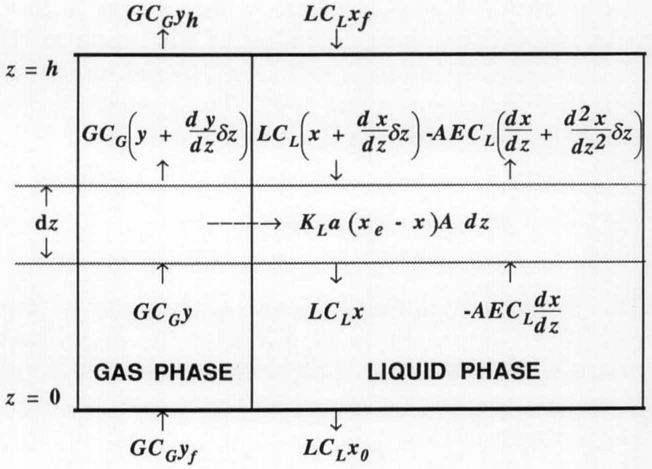

Figure 1. *Idealization of gas-liquid contacting in a packed column.*

solution for X must be of the form

$$X = c_1 e^{(d_1 w)} + c_2 e^{(d_2 w)} \tag{31}$$

where d_i are the roots of the characteristic equation

$$d_i = \frac{-\mathrm{Pe} \pm \sqrt{\mathrm{Pe}^2 + 4\,\mathrm{Pe}\,N}}{2} \tag{32}$$

The integration constants, c_i, are determined from application of the boundary conditions. The result is

$$c_1 = \frac{d_2\,\mathrm{Pe}\,X_f}{d_2(\mathrm{Pe}+d_1)\exp(d_1) - d_1(\mathrm{Pe}+d_2)\exp(d_2)} \tag{33}$$

$$c_2 = \frac{d_1\,\mathrm{Pe}\,X_f}{d_1(\mathrm{Pe}+d_2)\exp(d_2) - d_2(\mathrm{Pe}+d_1)\exp(d_1)} \tag{34}$$

The experimental results are applied to this solution to predict the overall mass transfer coefficient combined with the effective interfacial area per unit volume, K_La. The effects of axial dispersion on the overall mass transfer coefficient can be observed by comparison with predictions from the solution to the model for plug flow.

Plug Flow Model

In the case of plug flow, the second order term in Eq. (24) is dropped. The resulting transport equation can be integrated directly for dilute systems where the driving force (x_e - x) is a linear function in x. The solution is

$$N = \frac{K_L ahA}{LC_L} = \frac{(x_0 - x_f)}{(x_e - x)_{lm}} \tag{35}$$

where the log-mean driving force is defined as

$$(x_e - x)_{lm} = \frac{(x_e - x)_0 - (x_e - x)_f}{\ell n\left[\frac{(x_e - x)_0}{(x_e - x)_f}\right]} \tag{36}$$

The subscripts 0 and f indicate the conditions at z = 0 and h, respectively. The details for the derivation of Eq. (35) are found in Bennett and Myers.[5] The solution to the plug-flow model can also be obtained by solving the general model for large values of Pe.

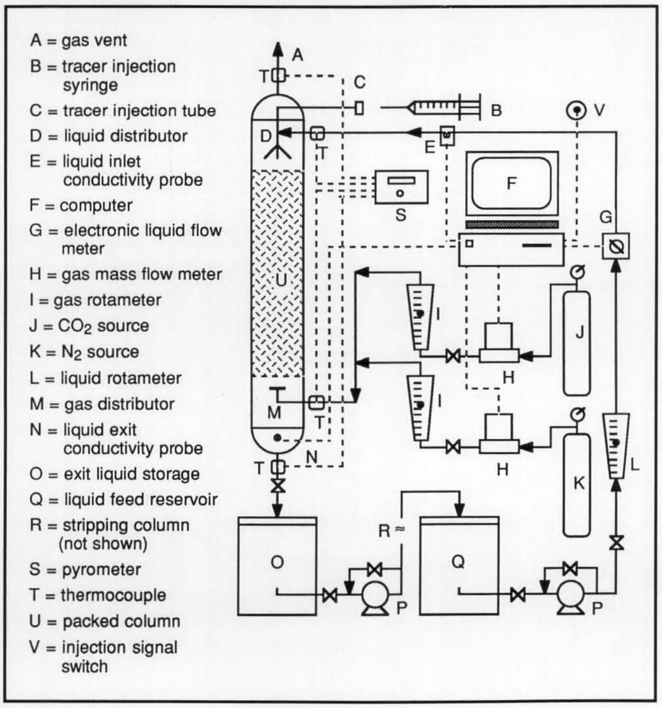

Figure 2. *Packed-column apparatus used in tracer and absorption experiments.*

APPARATUS AND PROCEDURE

A diagram of the apparatus is shown in Figure 2. The apparatus consists of two identical 4-inch inside diameter glass columns packed with 4 feet of 1/2-inch ceramic Intalox saddles. One column is used for gas-absorption experiments and the other for stripping operations. To conserve water, the columns are arranged so that water can circulate through both columns simultaneously in the case of absorption experiments. In the case of tracer experiments, water is pumped from a 30-gallon plastic storage tank to the top of the absorption column. The liquid feed is distributed evenly over the top of the packing and allowed to flow through the packing. The exit stream is collected in a separate 30-gallon holding tank. The liquid flow rate is measured with a rotameter and an electronic flow meter. The flow rate is controlled by a valve that restricts liquid recirculation to the pump. The lower limit on the liquid flow rate is approximately two gallons per minute. Below this limit we found that the packing did not completely wet. The upper limit is set at approximately four gallons per minute to avoid flooding. Custom conductivity probes by Microelectrodes® are situated in the liquid feed and exit streams just above and below the packing to determine the inlet and exit liquid concentrations. The conductivity probes are situated so that a mixing-cup measurement is obtained at the exit stream of the liquid phase. CO_2 and N_2 gas are passed to the bottom of the packing through rotameters and electronic mass flow meters. The gas flow rates are controlled by needle valves. The temperatures of the gas/liquid feed and exit streams are measured with thermocouples. An IBM personal computer is used to monitor the gas/liquid flow rates and the liquid conductivities. The software Labtech Notebook® is used to collect and display the signals from the column on the computer. The data are imported directly to the spreadsheet program Lotus 123® for manipulation and analysis.

The procedure for the gas absorption experiment consists of setting the gas and liquid flow rates and monitoring the liquid-phase conductivities until a steady state is reached. The conductivity probes are calibrated against aqueous CO_2 solutions with known concentrations by titration. Each student group carries out its own calibration. The CO_2 is fixed in solution by adding excess NaOH, then precipitated with $BaCl_2$. The excess NaOH is titrated with HCl. Pure CO_2 gas was used in the absorption column to avoid gas-phase dispersion effects. The stripping column uses N_2 gas.

In the case of tracer experiments, the conductivity of the liquid is monitored to achieve a base line. Approximately 1 ml of 5 M HCl is injected through a 1/16-inch ID Teflon tube into the liquid feed just before the liquid distributor at the top of the column. The volume of the injection tube is approximately 1 ml. A rubber septum caps the end of the injection tube in order to prevent tracer fluid from being forced back out of the tube, and an electric switch is provided to record the beginning and duration of the tracer injection period. It can be assumed that the initial perturbation approaches an impulse or delta function if the time period of the tracer injection is small relative to the time span for the signal at the bottom of the column. With the arrangement described here, we found that it required approximately 0.25 seconds to inject the tracer. This may be compared to mean residence times greater than 20 seconds. The conductivity data of the liquid exit stream are collected until the value of response returns to the base line. The conductivity of HCl was found to be a linear function of concentration over the range of conditions for this experiment. Therefore, it is unnecessary to calibrate the conductivity probes for HCl because the response to the tracer is normalized for the total amount of tracer injected.

ANALYSIS OF RESULTS

The analysis has two parts: calculation of the dispersion coefficient, and calculation of the overall liquid-phase mass transfer coefficient combined with the effective interfacial area per unit volume. A computer spreadsheet is used to convert the tracer-experiment data to a usable form.

The RTDs from tracer experiments are used with the dispersion model to obtain a dispersion number. It must be assumed that the tracer injection is an ideal impulse perturbation because the variance at the top of the column cannot be obtained experimentally from our arrangement. For either small or large extents of dispersion, it is necessary to calculate the variance of the RTD for the tracer at the liquid exit. Initially, the baseline concentration signal is subtracted from all the concentration data. The mean residence time and variance are obtained from the

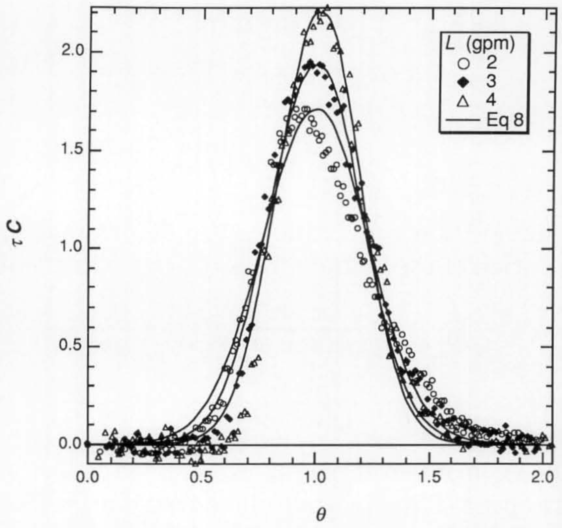

Figure 3. *C curves from tracer experiments compared with the small extent of dispersion model*

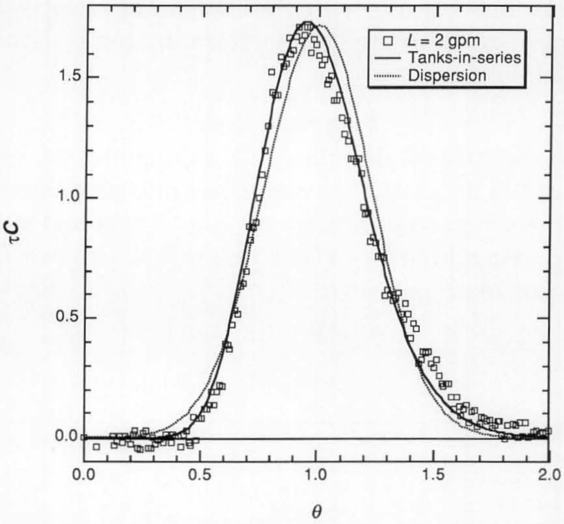

Figure 4. *Comparison of tanks-in-series and the small extent of dispersion models for intermediate-to-large extent of dispersion.*

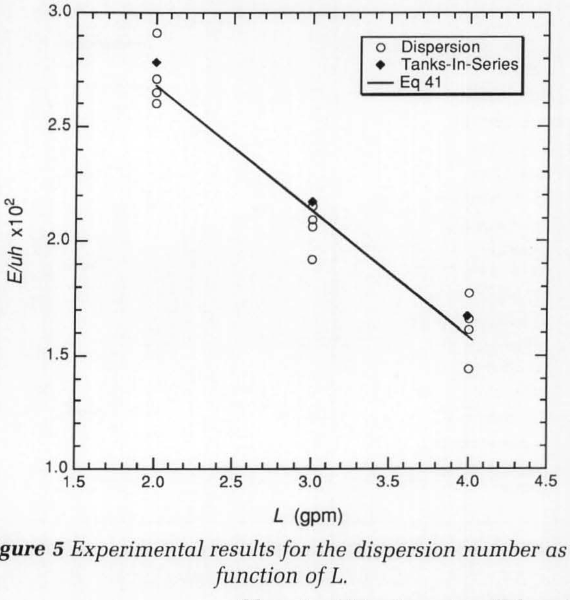

Figure 5 *Experimental results for the dispersion number as a function of L.*

discrete concentration vs time data according to the following approximations[1]

$$Q \cong \sum_{i=1}^{N} C_i \Delta t \tag{37}$$

$$\mathbf{C}_i \cong \frac{C_i}{Q} \tag{38}$$

$$\tau \cong \sum_{i=1}^{N} t_i \, \mathbf{C}_i \Delta t \tag{39}$$

$$\sigma^2 \cong \sum_{i=1}^{N} t_i^2 \, \mathbf{C}_i \Delta t - \tau^2 \tag{40}$$

where Δt is the time interval between sampling, and N is the number of data pairs. Experimental **C** curves are plotted in Figure 3 for three liquid flow rates. Care must be taken when applying Eqs. (37) to (40) to the experimental data. The final results may depend on the choice of the last data point due to the scatter in the measurements around the base line. When this is difficult, Levenspiel[2] suggests drawing a curve through the data by hand and picking points at uniform intervals from the curve.

The dispersion numbers were determined from Eqs. (9), (12), or (13), depending on the extent of dispersion. The criteria for determining the extent of dispersion is based on the shape of the **C** curve. As seen in Figure 3, there is little dispersion for liquid flow rates of 3 and 4 gallons per minute. At 2 gallons per minute, the shape of the **C** curve begins to deviate from the symmetric Gaussian distribution of Eq. (8), indicating a larger extent of dispersion. The TIS model was found to fit the data better than the small dispersion model at this low flow rate. Both models are compared in Figure 4. A numerical solution of Eq. (2) is necessary to obtain the dispersion model **C** curve for large extents of dispersion. This is beyond the scope of the present experiment.

TABLE 1

Comparison of K_La from Plug Flow and Dispersion Models
$T = 24°C$; $P = 1$ atm; $x_e = 0.00060$;[7] $G = 10$ L/min

$L\left(\frac{gal}{min}\right)$	x_f	x_o	E/uh	$K_La\left(\frac{lbmol}{ft^3 \cdot hr}\right)$ Dispersion	Plug Flow	% Deviation
2.0	0.00012	0.00049	0.027	243	234	3.7
3.0	0.00016	0.00049	0.022	340	330	2.9
4.0	0.00017	0.00048	0.016	414	405	2.2

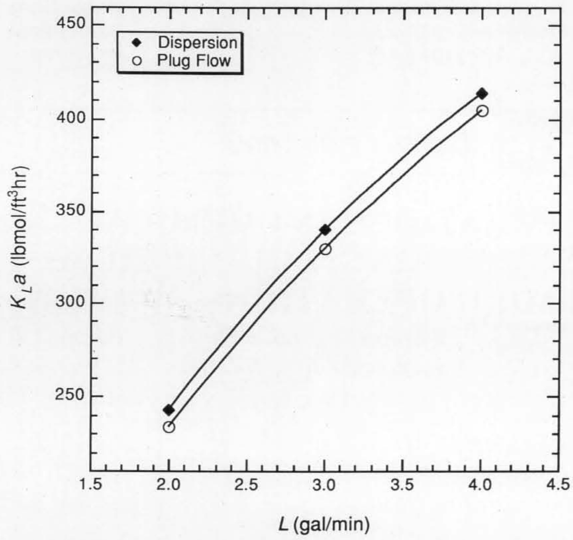

Figure 6. *Comparison of K_La from plug flow and dispersion models.*

In order to demonstrate the procedure, four tracer experiments were performed at each of the three flow rates above. The experimental results for the dispersion number from the dispersion and TIS models are plotted in Figure 5. They indicate small-to-intermediate amounts of dispersion in the packed column. For this limited range of operating conditions, the results for the dispersion number from the dispersion model can be correlated by a least-squares method to Eq. (41)

$$\frac{E}{uh} = 0.038 - 0.0055\,L(\text{gpm}) \tag{41}$$

A similar correlation was found from the TIS results for the dispersion number. The dispersion number is a decreasing function of liquid flow rate. This indicates that plug flow conditions are approached as the liquid flow rate increases. This may be due to a decrease of liquid stagnation in the packing at higher flow rates.[6]

Dispersion numbers from Eq. (41) are used in the differential model to predict K_La, assuming the tracer measurements are valid under mass-transfer conditions. This is probably a good assumption in this case since a relatively small quantity of CO_2 is absorbed. The non-linear transport equation for the liquid phase, Eq. (31), is readily solved for K_La by application of Newton's method with a computer. The solution method requires guessing values for K_La until the calculated exit conditions match the experimental results for the liquid-phase exit concentration. The experimental data and results are listed in Table 1 and the calculations for K_La are compared with the plug-flow case in Figure 6. The largest deviation from the plug-flow model was found to be approximately 4%. It is important to note that dispersion in the liquid phase has a negative effect on gas absorption. This is demonstrated here by the difference in magnitude of K_La for each case. K_La for the dispersion model must be larger to achieve the same separation as the plug-flow model.

DISCUSSION

The results from the analysis reveal that, for our absorption column, dispersion effects are small over the range of operating conditions reported. Thus, the plug-flow assumption is valid in this case, and the analysis of the mass transfer coefficient is simple. Often, simplifying assumptions are presented without justification. This new experiment provides students with the opportunity to verify the assumptions that are used to derive the well-known result for the mass transfer coefficient in a packed column. In this paper we chose to present the differential model as the one most closely representing the physical characteristics of the flow pattern through the packing. The students are not limited, however, to this model to explain deviations from plug flow. Levenspiel,[1] Lo, *et al.*,[4] and King[3] describe several models used for this purpose. For small-to-intermediate extents of dispersion, a tanks-in-series model with back flow is commonly employed. Other models use recirculation, back mixing, dead volumes, and combinations of these in conjunction with the tanks-in-series model. These models are much more cumbersome, and we found the dispersion and the tanks-in-series models adequate for our purposes.

The apparatus described here was designed at UCSB and was constructed by an off-campus contractor at a cost of $12,000. The electronic instrumentation was an additional $6,000. The apparatus is used in each of our required two-quarter sequence courses in Chemical Engineering Laboratory. In the first-quarter course, steady-state data are taken to determine mass transfer coefficients, and in the second quarter the axial dispersion measurements described here are carried out.

ACKNOWLEDGEMENT

The authors benefitted from many enlightening discussions with Professor R.G. Rinker regarding the modeling of dispersion. This work was sponsored by a Teaching Assistant Instructional Grant funded by the UCSB Instructional Improvement Program.

NOMENCLATURE

a = interfacial area per unit volume, ft^{-1}
A = cross-sectional area of empty column, ft^2
c_i = integration constants, Eqs. (33) and (34)
C = concentration, $lbmol \cdot ft^{-3}$
$\mathbf{C}$ = normalized concentration, s^{-1}
d_i = roots to characteristic equation, Eq. (32)
E = dispersion coefficient, $ft^2 \cdot s^{-1}$
G = volumetric gas flow rate, $ft^3 \cdot hr^{-1}$
h = column height, ft
K_L = liquid phase overall mass transfer coefficient, $lbmol \cdot ft^{-2} \cdot s^{-1}$
L = volumetric liquid flow rate, $ft^3 \cdot hr^{-1}$
m = equilibrium coefficient
N = dimensionless group, Eq. (28), or number of data pairs
n = number of tanks in tanks-in-series model
P = pressure of the gas phase, atm
Pe = Peclet number, Eq. (27)
Q = total tracer response integrated over all time
t = time, s
u = linear velocity of the liquid, $ft \cdot hr^{-1}$
w = dimensionless length, z/h
X = $x_e - x$
x = mole fraction of solute in the liquid phase
y = mole fraction of solute in the gas phase
z = axial coordinate, ft

- ***Greek Symbols***

σ = standard deviation
θ = dimensionless time
τ = mean residence time, s

- ***Subscripts***

e = equilibrium condition
f = feed condition
h = top of column
G = gas phase
L = liquid phase
lm = log mean driving force, Eq. (36)
0 = bottom of column

REFERENCES

1. Levenspiel, O., *Chemical Reaction Engineering,* John Wiley & Sons, New York, pp 253-304 (1972)
2. Levenspiel, O., *The Chemical Reactor Omnibook,* Oregon State University Bookstores, Inc., Corvallis, OR, Ch. 64-66 (1979)
3. King, C.J., *Separation Processes,* McGraw-Hill, New York, pp 570-573 (1980)
4. Lo, T.C., M.H. Baird, and C. Hanson, eds., *Handbook of Solvent Extraction,* John Wiley & Sons, New York, pp 201-203 (1983)
5. Bennett, C.O., and J.E. Myers, *Momentum, Heat and Mass Transfer,* McGraw-Hill, New York, pp 541-545 (1982)
6. Van Swaaij, W.P.M., J.C. Charpentier, and J. Villermaux, "Residence Time Distribution in the Liquid Phase of Trickle Flow in Packed Columns," *Chem. Eng. Sci.,* **24**, 1083 (1969)
7. Henley, E.J., and J.D. Seader, *Equilibrium-Stage Separation Operations in Chemical Engineering,* John Wiley & Sons, New York, 124 (1981) ❐

ChE book review

SEPARATIONS IN CHEMICAL ENGINEERING: EQUILIBRIUM STAGED OPERATIONS

by Phillip C. Wankat; Prentice Hall Publishing Co., 113 Silvan Ave., Englewood Cliffs, NJ 07632; 707 pages, $47.50 (1988) (Formerly published by Elsevier Publishing Co.)

Reviewed by
Roseanne M. Ford
University of Virginia

Engineering analysis and design of the classical separation methods of distillation, absorption, and